Supplemental Figure 1

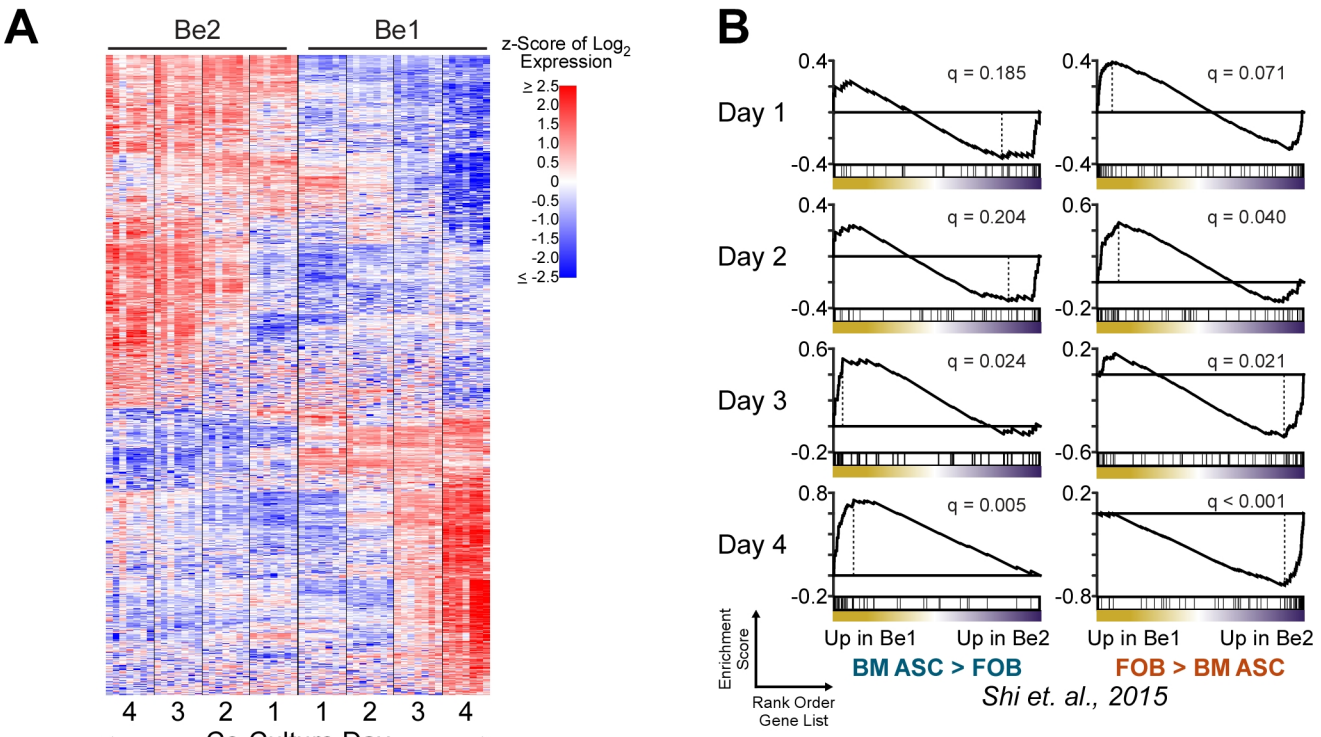

Figure S1. Be1 cells upregulate Blimp1 by day 2 and commit to the ASC lineage between days 2-3 (related to Fig. 1).

(A) Expression on days 1-4 of 760 genes (1022 probe sets) that exhibited a ≥2-fold change and FDR<0.05 between day 4 Be1 and Be2 from Affymetrix microarray (MA) data sets. Heat map showing clustered gene expression patterns over time (see also Table S1). Color corresponds to Z-score (per gene) of $\log_2$ expression. Euclidean distance and average linkage were used for clustering.

B) GSEA plots of days 1-4 Be1 and Be2 cell MA data sets compared to TF genes reported (Shi et al., 2015) to be significantly upregulated in BM ASC or FOB. Enrichment score (ES) is plotted against the ranked gene list (n = 17186) for TF genes upregulated in BM ASC (left) or FOB (right). Dashed vertical lines indicates the cutoff for leading edge genes. See also Fig. 1G.

C) Volcano plots of Be1 and Be2 MA data showing DEGs on days 1-4 based on q<0.05 and ≥1.75-fold change cutoff. TFs differentially expressed in BM ASCs (blue) and FOB (red) (Shi et al., 2015) are indicated. See also Fig. 1H.

MA analysis was performed with seven independent experimental samples/group/timepoint. FDR *q* values (B) computed based on 1000 random phenotype permutations.

Supplemental Figure 2

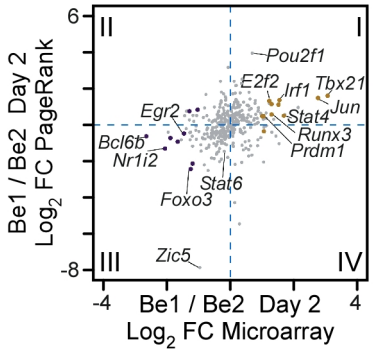

Figure S2. PageRank analysis predicts TF activity in day 2 Be1 and Be2 cells (related to Fig. 2). Assignment of TFs to Be1 (gold) or Be2 (purple) network by PageRank analysis (Yu et al., 2017). Log_2 fold change in expression of genes by MA (X axis) is plotted against the log_2 fold change in the Be1 versus the Be2 PageRank statistic (Y axis). In quadrant I, genes shown in gold were assigned to the Be1 PageRank network, based on having both a positive log_2FC by PageRank statistic and log_2FC of > 1 and FDR < 0.05 by MA. In quadrant III, genes shown in purple were assigned to the Be2 PageRank network based on both a negative log_2FC by PageRank statistic and log_2FC of < -1 and FDR < 0.05 by MA (See also Fig. 2A and Table S3).

Supplemental Figure 3

A

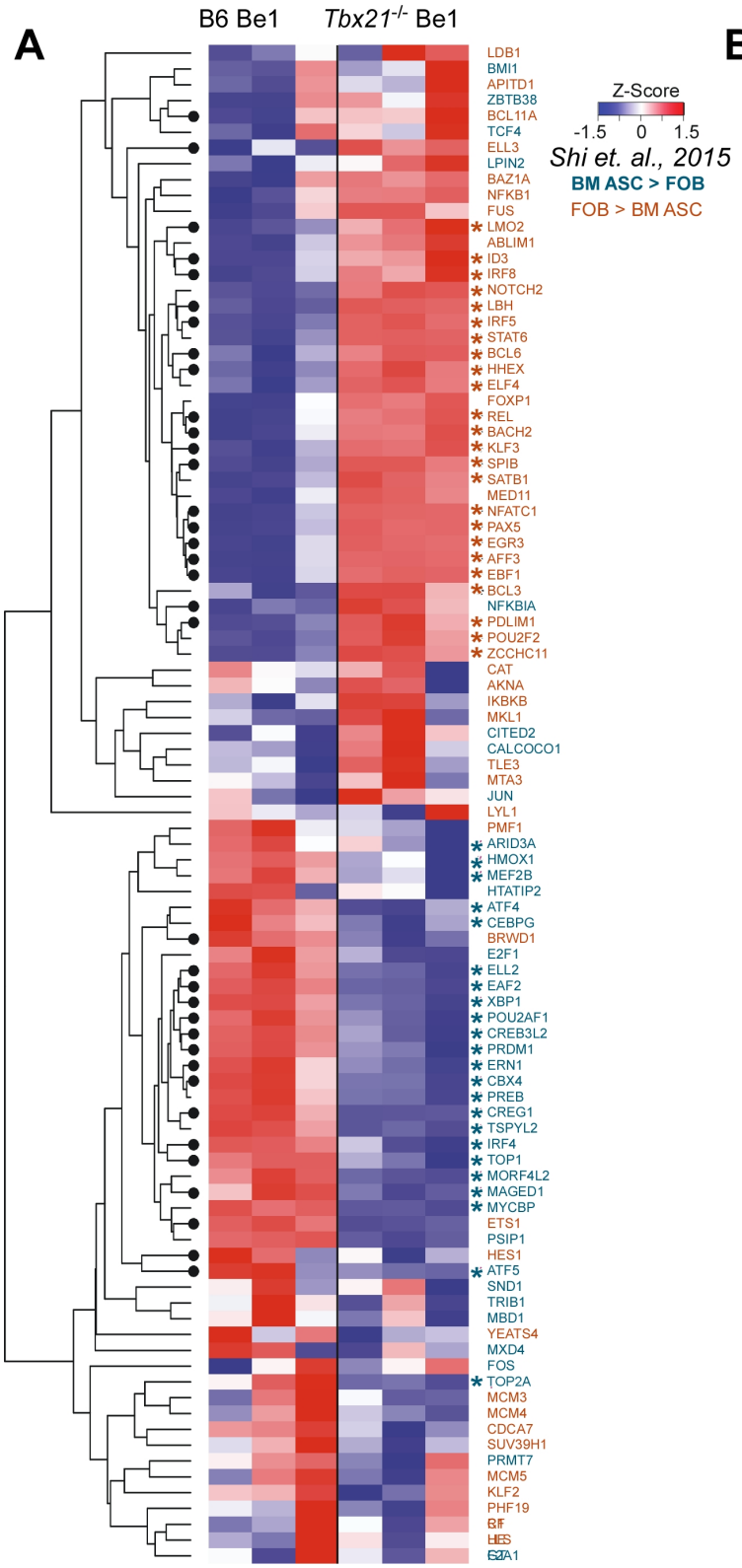

B

Transcription Factor	B6 Be1 vs B6 Be2 *p* value	B6 Be1 vs *Tbx21*$^{-/-}$ Be1 *p* value
Tbet	1.6 e-68	1.3 e-68
Blimp1	3.8 e-90	0.48
Pax5	5.6 e-6	0.042
SpiB	2.2 e-16	4.2 e-8
BCL6	4.6 e-6	0.23
XBP1	0.035	0.14
IRF4	1.5 e-53	0.005
OCT2	8.6 e-6	0.002

Figure S3. T-bet regulates ASC development in Be1 cells (related to Fig. 3).

A) Heat map showing expression levels of 96 TF genes that were previously defined as differentially expressed in BM ASC and FOB (Shi et al., 2015) and were also present in the Day 4 B6 and *Tbx21*$^{-/-}$ Be1 cell RNA-seq data sets. Heat map color corresponds to Z-score of $\log_2$ expression of day 4 B6 and *Tbx21*$^{-/-}$ Be1 samples from the RNA-seq data set (n= 3 independent biological samples/group). Solid circles on dendrogram indicate genes that exhibited a ≥2 FC in expression and q<0.05 between day 4 B6 and *Tbx21*$^{-/-}$ Be1 cells. (n=3/group). Genes labeled in blue font (41 genes) are those reported to be more highly expressed in BM ASC relative to FOB and genes labeled in red font (55 genes) are those reported to be more highly expressed in FOB relative to BM ASCs (Shi et al., 2015). Asterisks indicate leading edge genes based on GSEA. See also Fig. 3D-E and Table S4.

(B) *p* values for Fig. 3G, chromatin accessibility at transcription factor consensus DNA binding motifs in ATAC-seq data (See also Table S4).

RNA-seq and ATAC-seq analysis was performed with 3 independent samples/group.

Supplemental Figure 4

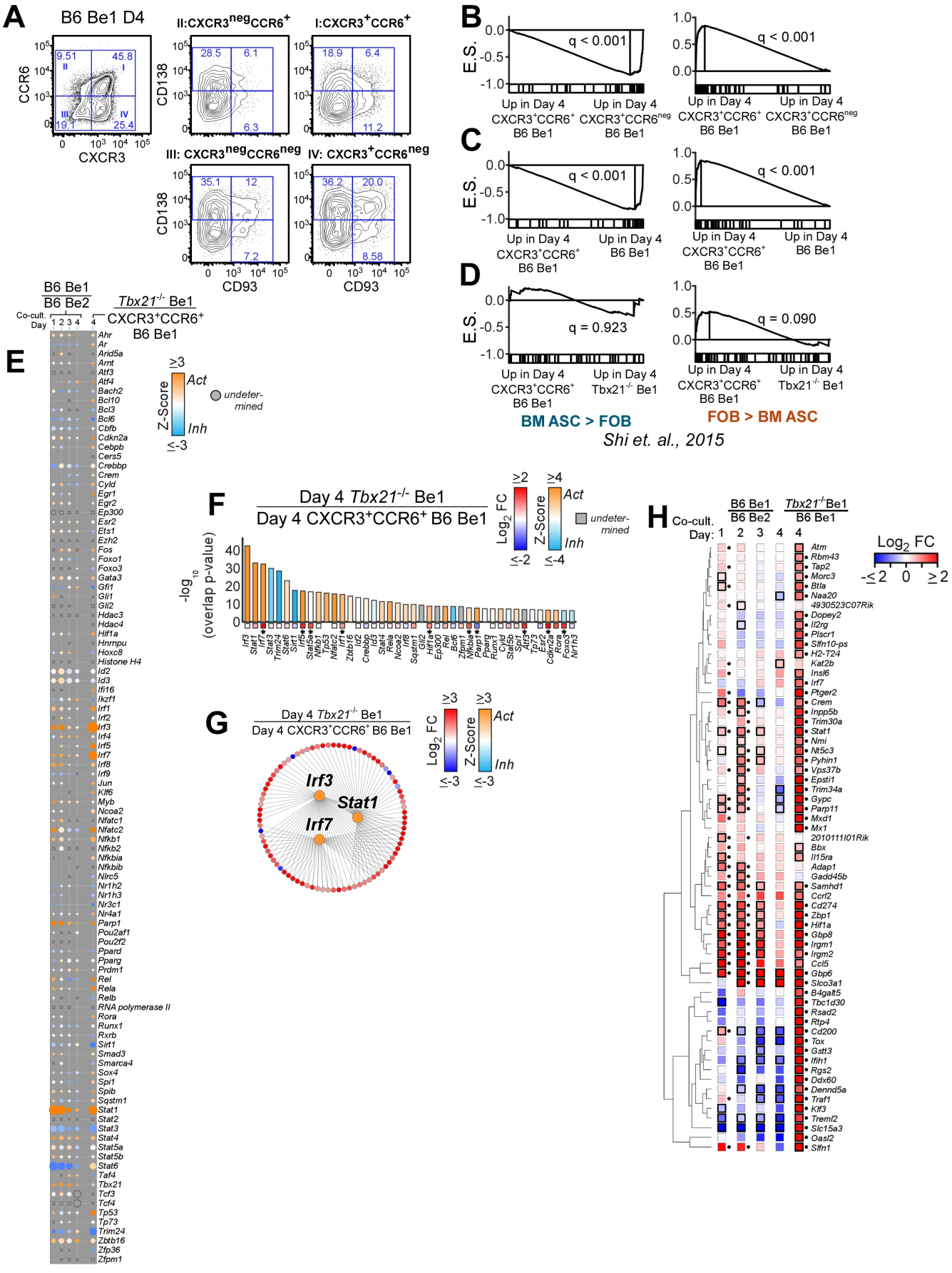

Figure S4. T-bet represses the IRF and STAT induced inflammatory signature in Be1 cells (related to Fig. 4).

(A-D) Identification of a non-ASC enriched effector cell population ($CXCR3^+CCR6^+$) in day 4 Be1 cultures. Expression of CXCR3 and CCR6 (A, left side) in B6 Be1 cells on day 4 of co-culture and expression of ASC markers CD93 and CD138 within the CXCR3 and CCR6 subsets (A, right side). Frequency of cells within gated regions are noted. GSEA plots (B-D) comparing day 4 total Be1, $CXCR3^+CCR6^+$ effector Be1, $CXCR3^+CCR6^{neg}$ Be1 and *Tbx21*$^{-/-}$ Be1 to TF genes that are reported (Shi et al., 2015) to be significantly upregulated in BM ASC or FOB. Enrichment score (ES) is plotted against the ranked gene list for TF genes upregulated in BM ASC (left) or FOB (right). Dashed vertical lines indicates the cutoff for leading edge genes. GSEA reveals that day 4 $CXCR3^+CCR6^{neg}$ cells are enriched in BM ASC TFs relative to the $CXCR3^+CCR6^+$ effector cells, suggesting that the $CXCR3^+CCR6^+$ population contains fewer ASCs than the $CXCR3^+CCR6^{neg}$ population. Consistent with this conclusion, Day 4 $CXCR3^+CCR6^+$ effector Be1 cells are enriched in FOB TF genes when compared to the $CXCR3^+CCR6^{neg}$ subset or the total Be1 cells. Moreover, $CXCR3^+CCR6^+$ effector Be1 cells and the *Tbx21*$^{-/-}$ Be1 cells show similar low expression of BM ASC TFs and GSEA reveals no significant enrichment in expression of the ASC (or FOB) defined TFs between the $CXCR3^+CCR6^+$ effector Be1 cells and *Tbx21*$^{-/-}$ Be1 cells. See Table S4 for detailed transcriptional profiling showing that the $CXCR3^+CCR6^+$ "effector" subset of Be1 cells is predominantly composed of non-ASC effector populations.

(E-G) IPA upstream regulator analysis of RNA-seq data from day 4 *Tbx21*$^{-/-}$ and B6 $CXCR3^+CCR6^+$ effector Be1 cells and MA data from days 1-4 Be1 and Be2 cells. Heatmap (E) of activation Z-scores (activated (Act), orange; inhibited (Inh), blue; or undetermined, grey) for TFs predicted by IPA to be upstream regulators of B6 Be1 over B6 Be2 (days 1-4) or day 4 *Tbx21*$^{-/-}$ Be1 over day 4 B6 $CXCR3^+CCR6^+$ effector Be1 cells. Circle size is proportional to $-\log_{10}$ overlap *p* value. Top IPA predicted upstream regulators (F) from the day 4 *Tbx21*$^{-/-}$ over day 4 B6 $CXCR3^+CCR6^+$ effector Be1 cells comparison ranked by overlap *p* value, colored by activation Z-score. Squares below bars indicate $\log_2$ FC in expression for each predicted regulator with * indicating FDR <0.05. Regulator-target circular graphs (G) based on IPA upstream regulator analysis of Day 4 *Tbx21*$^{-/-}$ Be1 over Day 4 B6 $CXCR3^+CCR6^+$ effector Be1 cells. Shown are 3 selected predicted upstream regulators (center; *Irf3*, *Irf7*, *Stat1*) and their target genes (outer circle) with lines connecting regulators to target genes. Predicted regulators are colored by Z-score and target genes by $\log_2$ FC in expression determined from RNA-seq datasets. (see also Table S5 and Fig. 4A-C).

(H) Expression of genes, which are reported to be direct targets of T-bet repression in Th1 cells, in Be1 cells. Heat map display of leading edge genes identified in the GSEA comparison (see Fig. 4J-L) of day 1 Be1 vs Be2, day 2 Be1 vs Be2 and day 4 *Tbx21*$^{-/-}$ Be1 vs B6 Be1 to genes that were reported to be repressed and bound by T-bet in day 4 Th1 cells (Iwata et al., 2017). Data shown as FC ($\log_2$

expression ratio of MA data Be1 over Be2 days 1-4 and RNA-seq data *Tbx21*$^{-/-}$ Be1 over B6 Be1 day 4) with black borders indicating q < .05 for the corresponding differential expression comparison, and black dots indicating membership in the leading-edge subset for the corresponding GSEA analysis. Genes were clustered based on Euclidean distance of the fold-change data and complete linkage.

Data shown are representative of 3 independent experiments (A). RNA-seq analysis was performed with 3 *Tbx21*$^{-/-}$ Be1, 1 CXCR3^{+}CCR6^{+} B6 Be1, 1 CXCR3^{+}CCR6^{neg} B6 Be1, and 3 day 4 B6 Be1 samples. MA analysis was performed with 7 samples/group/timepoint. Statistical significance between samples was determined using FDR *p* analyses (E-G) or FDR q analyses (B-D). Genes which had on overlap *p* value <0.05 by IPA were predicted to be upstream regulators (E-G).

Supplemental Figure 5

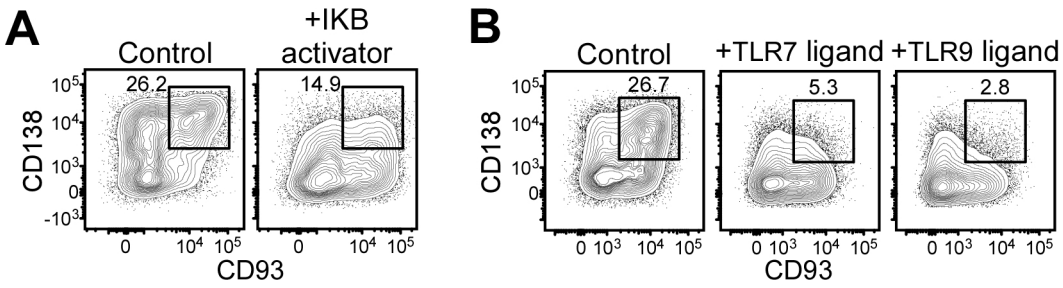

Figure S5. Sustained TLR and NF-κB signaling prevents ASC development in Be1 cultures (related to Fig. 5).

(A) Vehicle or IKK/NF-κB, Betulinic acid, was added to day 2 B6 Be1 cultures generated as in Fig. 1. On day 4 ASCs were quantified as $CD138^{+}CD93^{+}$ cells by flow cytometry. (See also Fig. 5A).

(B) Vehicle, TLR7 ligand R848, or TLR9 ligand CpG, was added to day 2 B6 Be1 cultures. On day 4 ASCs were identified as $CD138^{+}CD93^{+}$ cells by flow cytometry. (See also Fig. 5C).

Data shown are representative of 3 independent experiments.

Supplemental Figure 6

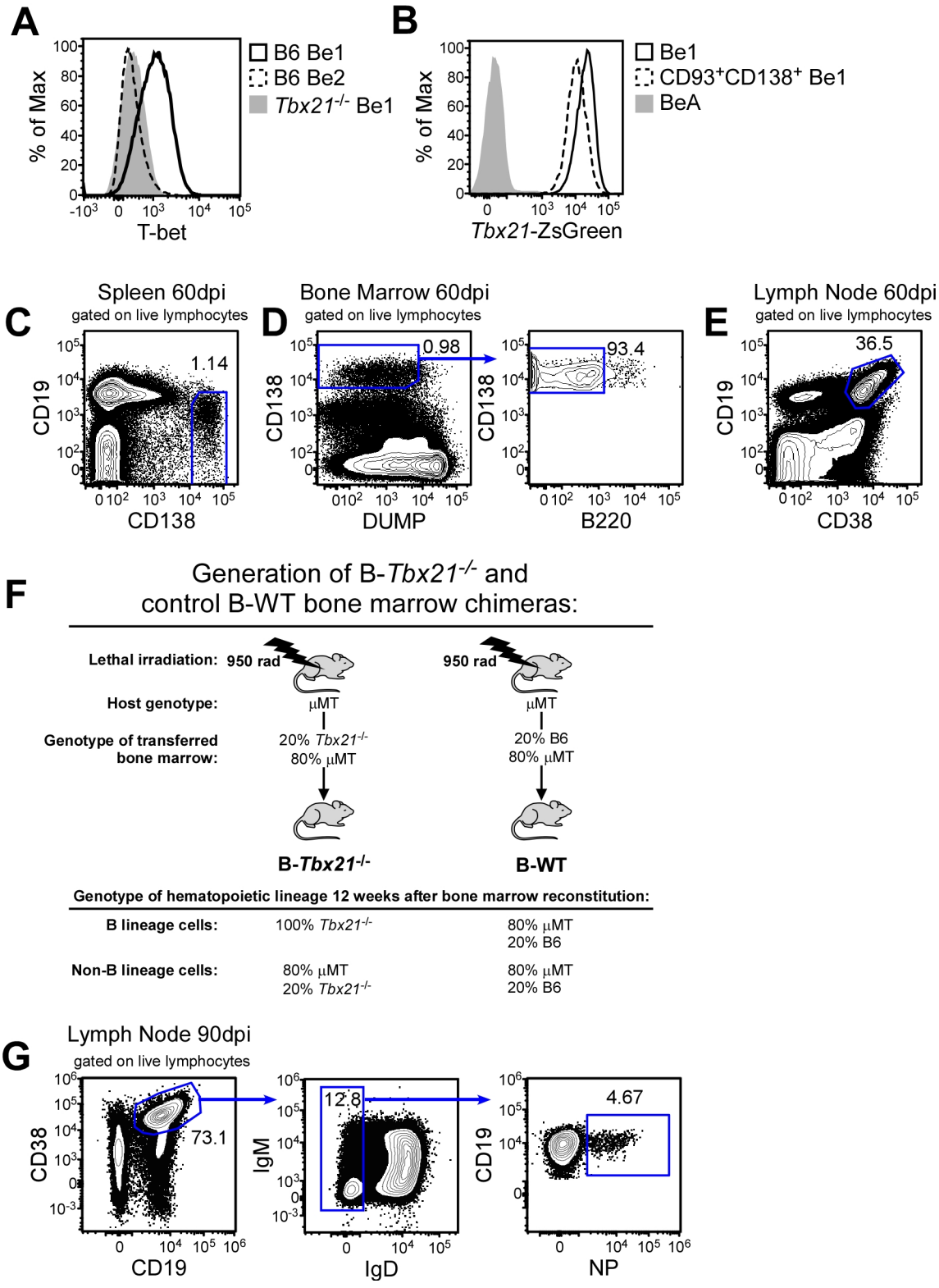

Figure S6. Identification of T-bet expressing B cells in flu-infected T-bet reporter mice and B cell bone marrow chimeras (related to Fig. 6).

(A-B) T-bet expression in B effector cultures. T-bet protein levels (A) as measured by intracellular staining in B6 Be1, B6 Be2, and *Tbx21*$^{-/-}$ Be1 cells on day 4 of co-culture. (B) Representative histograms showing T-bet-ZsGreen reporter expression in day 4 Be1 cells and CD138^{+} CD93^{+} Be1 cells, gated as in Fig. 1A.

(C-E) Gating strategies to identify B cell subsets in T-bet-ZsGreen reporter mice 60 days post-PR8 infection. Gating to identify splenic plasma cells ((C), see also Fig. 6D), bone marrow plasma cells ((D) see also Fig. 6E) and LN CD38^{+}CD19^{+} cells ((E), see also Fig. 6F-G). Dump channel includes CD3, CD4, CD43, NK1.1, Ly6G, and Ter119.

(F) Cartoon showing generation of bone marrow chimeric mice harboring *Tbx21*$^{-/-}$ B cells (B-*Tbx21*$^{-/-}$ mice), and control chimeras with WT B cells (B-WT mice). Top, recipient (host) μMT mice were lethally irradiated (950 rad) prior to adoptive transfer of a mixture of bone marrow cells, as depicted. Bottom, genotype of hematopoietic cells after allowing 12 weeks for engraftment of transferred bone marrow.

(G) Gating strategy to identify NP^{+}CD38^{+}IgD^{neg} memory B cells (BMEM) in LN of B-WT mice 90 days post-infection (See also Fig. 6P). Shown in the far-right panel are 9700 cells.

Representative data from one of 3 independent experiments with 3-4 experimental replicates (A-B) or 3-5 mice (C-E, G) per group.

Supplemental Figure 7

A

Treatment Groups		Treatments Administered: 1° infection PR8	Treatments Administered: Tamoxifen Treatment 90dp PR8	Treatments Administered: 2° infection X31 (*if assessing memory recall*)	Effect of Tamoxifen Treatment on B memory cells	Purpose of control
Experimental Group	***Tbx21*$^{fl/fl}$.CD20-TAM-Cre + TAM**	X	X	X	T-bet deficient B memory cells	**N/A**
Control Groups	**CD20-TAM-Cre + TAM**	X	X	X	WT B memory cells	Effect of tamoxifen-induced Cre activity in CD20+ cells
	B6 + TAM	X	X	X		Effect of Tamoxifen on non-transgenic cells
	B6 X31 1° infection control			X	N/A (lacks B memory cells)	Lacks pre-formed PR8-specific memory cells & antibodies

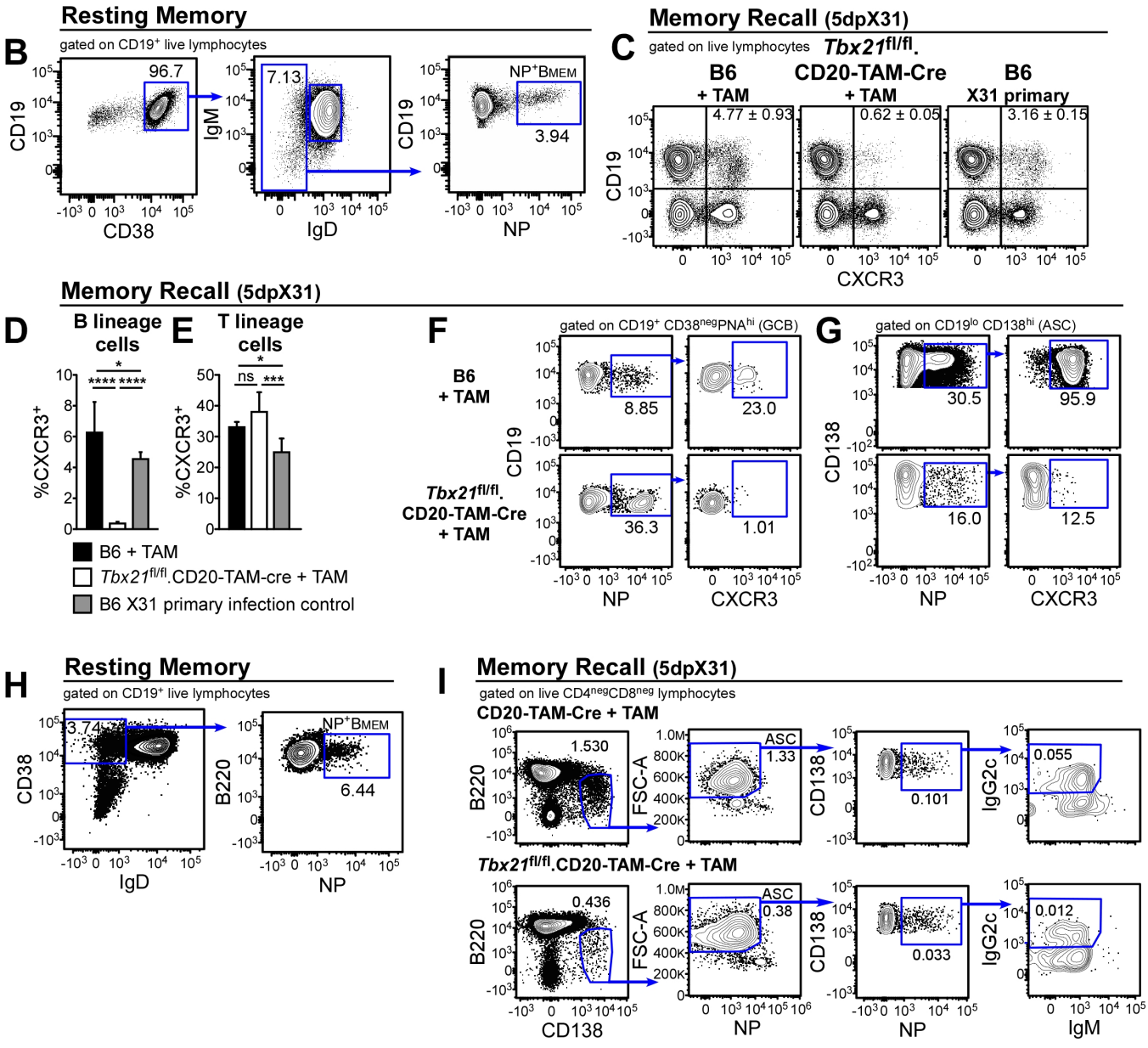

Figure S7. Identification of B cell subsets following induced deletion of *Tbx21* in memory B cells (related to Fig. 7)

(A) Table depicting experimental design and rationale for controls in experiments designed to assess the effect of induced *Tbx21* deletion in memory B cells (BMEM) after establishment of the memory B cell compartment (see also Fig. 7A). Following *Tbx21* deletion in BMEM cells of flu memory mice, analyses were performed on the resting flu-specific BMEM compartment (see Fig. 7B-F and J-L). Alternatively, following *Tbx21* deletion in BMEM cells of flu memory mice, mice were challenged with a heterosubtypic influenza virus and the BMEM-derived flu-specific GCB and ASC responses were measured (see Fig. 7G-I and M).

(B) Gating strategy to identify $NP^{+}CD38^{+}IgD^{neg}$ memory B cells (BMEM) following inducible deletion of *Tbx21* in LN BMEM cells (See also Fig. 7E).

(C-E) CXCR3 expression by T and B lineage LN cells on day 5 post-challenge flu infection in tamoxifen-treated memory recall B6 and $Tbx21^{fl/fl}$.CD20-TAM-Cre mice and primary infected B6 mice. Example flow plots (C) and the frequency of $CXCR3^{+}$ B lineage cells (sum of $CD19^{+}$ $CD138^{neg}$ B cells and $CD19^{lo}CD138^{hi}$ ASCs) (D) and $CXCR3^{+}$ $CD3^{+}$ T lineage cells (E).

(F-G) Gating strategy to identify $NP^{+}CXCR3^{+}$ GCB (F) and ASC (G) 5 days after X31 challenge infection, pregated on total ASC and GCB (see Fig. 6A for pre-gates). See also Fig. 7G-I for quantitation.

(H) Gating strategy to identify $NP^{+}CD38^{+}IgD^{neg}$ BMEM cells. See also Fig. 7J-L for quantitation of flu-specific BMEM subsets.

(I) Gating strategy to identify $NP^{+}IgG2c^{+}$ ASC 5 days after X31 challenge infection. The frequency of each gated population within the total live lymphocyte population is indicated. See also Fig. 7M for quantitation.

Representative data from one of 2 (I) 3 (B-H) independent experiments, shown as the mean + SD of 3-6 mice/group. *p* values were determined using one-way ANOVA *$p<0.05$, ***$p\leq0.001$,****$p\leq0.0001$ or "ns" not significant.